Anilinolysis of Picryl Benzoate Derivatives in Methanol: Reactivity, Regioselectivity, Kinetics, and Mechanism

MAHMOUD F. IBRAHIM, MOHAMED A. EL-ATAWY, SAMIR K. EL-SADANY, EZZAT A. HAMED

Chemistry Department, Faculty of Science, Alexandria University, Alexandria 21321, Egypt

Received 3 August 2012; revised 9 November 2012; accepted 8 January 2013

DOI 10.1002/kin.20779
Published online 23 July 2013 in Wiley Online Library (wileyonlinelibrary.com).

ABSTRACT:: The reaction of picryl benzoate derivatives **1a–g** with aniline in methanol proceeds through CO–O and Ar–O bond cleavage pathways. Furthermore, the reactivity of these esters toward anilinolysis is correlated to the energy gap between highest occupied molecular orbital aniline and lowest unoccupied molecular orbital of each ester. The regioselectivity of acyl–oxygen versus aryl–oxygen cleavage is also discussed. The overall rate constants k_{tot} split into k_{CO-O} (the rate constant of acyl-oxygen cleavage) and k_{Ar-O} (rate constant of aryl-oxygen cleavage). The CO–O bond cleavage advances through a stepwise mechanism in which the formation of the tetrahedral intermediate is the rate-determining step. The Ar–O bond cleavage continues through a S_NAr mechanism in which the departure of the leaving group from the Meisenheimer complex occurs rapidly after its formation in the rate-determining step. © 2013 Wiley Periodicals, Inc. Int J Chem Kinet 45: 551–559, 2013

INTRODUCTION

The competition between the two electrophilic centers in the ester substrate is well documented for the reactions of nitrophenyl sulfonates, sulfates, and phosphates with a variety of nucleophiles [1,2]. Although carboxylic aryl esters mostly underwent acyl-oxygen cleavage [1a,3], partial Ar-oxygen cleavage was also reported, which is attributable to the strong activation of the 1-position (ipso) of the phenolic group by the nitro groups [4]. The acyl–oxygen bond or aryl–oxygen bond of phenyl esters can be cleaved depending on (i) the structure of the ester [5,6], (ii) the nature of reagent [4,7], (iii) the basicity of the leaving group anion from the ester compared to that of the attacking nucleophile, (iv) the nature of substituent in the nonleaving or leaving group containing the ester [4,7], and (v) the relative "hardness" and "softness" of the reaction site and reagent [8].

On the other hand, quantum chemistry provides many powerful tools, which facilitate in evaluating electron densities at different atoms of a molecule,

Correspondence to: Mahmoud F. Ibrahim; E-mail: mfawzy59@yahoo.com.

Supporting Information is available in the online issue at www.wileyonlinelibrary.com.

predicting the reaction sites, explaining the reactivity order of closely related reagents toward a given reaction center, and predicting the transition state structure [9]. In fact, the ester aminolysis is affected by the properties of the carbonyl group (C=O) and, so naturally, the ipso carbon of the phenolic part of ester. The authors report here the mechanisms for both the CO–O and Ar–O bond cleavage pathways for the reactions of picryl benzoates **1a–g** with aniline together with the effect of the benzoyl substituent on the reactivity, regioselectivity, and the reaction mechanism.

EXPERIMENTAL

Materials

The method of preparation and characterization of 2,4,6-trinitrophenyl x substituted benzoate has been described previously [10]. The purity of these esters was checked by means of their melting point and spectral data, such as IR and H NMR. Aniline was of the highest quality available and was distilled before use. The reaction medium was HPLC-grade methanol and was used as supplied.

Product Analysis

A methanolic solution (10 mL) of a given 2,4,6-trinitrophenylbenzoate derivatives **1a–g** and aniline was heated at the desired temperature for ca. 2 h. The reaction mixture was continuously checked (every 15 min) by TLC until the disappearance of the reactants spots. The workup afforded a mixture of four products, namely *N*-phenyl benzamide derivatives **2a–g**, anilinium picrate **3**, anilinium benzoate derivatives **4a–g**, and *N*-phenyl picramide **5**. All of these products were detected from TLC by comparing them with their authentic samples.

The reaction of a given substrate with aniline at the desired temperature under the same conditions of kinetic runs was followed. At the end of the reaction as indicated from TLC, the reaction mixture was subjected to HPLC measurements and the fractions of anilinium picrate and *N*-phenyl picramide for the reaction of aniline with esters **1a–g** at all the temperatures (20°, 25°, 30°, 35°, and 40°C) were determined.

The HPLC measurements were carried out on a Perkin–Elmer 200 series HPLC system including a quaternary pump, an injector with 20 μL sample, and a variable wavelength detector operated at 360 nm. The total chromatograph navigator software (version 6.2) was used for data acquisition. The stationary phase was a Spheri-5 RP-18, 220 mm i.d. cartridge packed with 5 μm particles (Brownlee columns). The flow rate was set at 1 mL min^{-1}. The mobile phases used were 51% methanol, 49% (v/v) 0.01 mol L^{-1} aqueous phosphate buffer at pH 3 (component A), and 100% methanol (component B). (The reported pH value is that of the aqueous solution before mixing with methanol.) Authentic samples of anilinium picrate (retention time = 2 min) and *N*-phenyl picramide (retention time = 11 min) were applied as a reference.

Kinetic Measurements

The reaction mixture was prepared by the transfer of 1 mL of the substrate solution that gave a final concentration of 1×10^{-4} M to a 10-mL measuring flask, and the volume was completed by a given volume of absolute methanol. The measuring flask and the stock solution of the aniline were allowed to reach a thermal equilibrium in a well-stirred and thermostatic bath at the desired temperature $\pm$ 0.5°C. The reaction time started when aniline was mixed with the reaction mixture (the final concentration of aniline ranged from 1×10^{-2} to 7×10^{-2} M) and transferred quickly to a well thermostatic chamber containing the UV cell. The absorbance A_t at the desired λ was recorded at several time intervals depending on the reaction rate. The resultant change in the absorbance with time was recorded in a kinetic mode on a UV–vis Shimadzu 160-A spectrophotometer. Measurements were usually carried out by following the increase in the absorbance of reaction products with time at $\lambda = 370$ nm.

Calculations

All calculations were performed using the GAUSSIAN 98 package [11] Calculations were made by DFT using Becke's three-parameter hybrid exchange functional in combination with the gradient-corrected correlation functional of Lee, Yang, and Parr B3LYP/ 6-31G** [12] methods.

RESULTS AND DISCUSSION

The anilinolysis of picryl benzoate derivatives **1a–g** in methanol proceed through a simultaneous acyl-oxygen and aryl-oxygen cleavage, as indicated by the isolation and identification of the reaction products, namely *N*-phenyl benzamide derivatives **2a–g**, anilinium picrate **3**, anilinium benzoate derivatives **4a–g,** and *N*-phenyl picramide **5** (Scheme 1). Therefore, the attacking sites of these esters **1a–g** are the

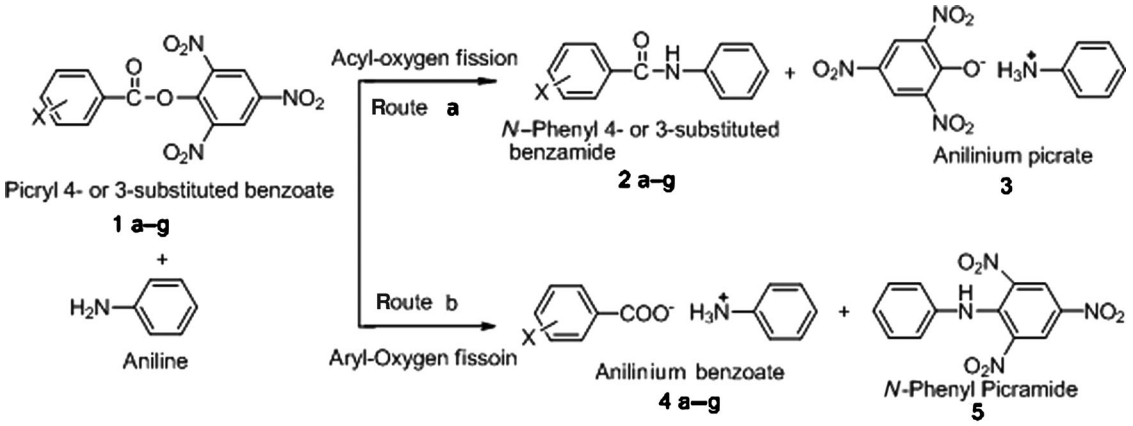

Scheme 1 a, X = H; b, X = 4-OCH_3; c, X = 4-CH_3; d, X = 3-CH_3; e, X = 4-Cl; f, X = 3-Cl; g, X = 4-NO_2.

carbonyl carbon atom (CO–O bond cleavage) and the trinitrophenyl ipso carbon atom (Ar–O bond cleavage). The fraction of anilinium picrate **3** was taken to determine the amount of acyl-oxygen cleavage and the fraction of *N*-phenyl picramide **5** account for the amount of aryl-oxygen cleavage. The percentages of CO–O and Ar–O are calculated by comparing the HPLC peak area of the reaction mixture with that of the authentic sample of anilinium picrate (retention time = 2 min) and N-phenyl picramide (retention time = 11 min), as shown in Table I. The results presented in Table I show that the CO–O cleavage (route a), which leads to the formation of *N*-phenyl benzamide derivative **2a–g** and anilinium picrate **3**, occurs dominantly for esters with the EWG in the benzoyl moiety. On the other hand, Ar–O cleavage (route b), which yields *N*-phenyl picramide **5** and anilinium benzoate derivatives **4a–g**, occurs considerably in the case of the reaction with the strong EDG in the benzoyl moiety of the ester.

Kinetics, Reactivity, and Regioselectivity for the Reaction of Picrylbenzoate Derivatives 1a–g with Aniline in Methanol

Kinetics. The rate of the anilinolysis was followed spectrophotometrically by observing the increase in the optical density near 370 nm due to the formation of both anilinium picrate **3** and *N*-phenyl picramide **5** while the other products had a negligible absorbance at this wavelength. In addition, the kinetic study was measured under pseudo–first-order conditions with the concentration of aniline maintained in excess relative to the ester concentration. The pseudo–first-order rate constants (k_{obs}) were calculated from the equation ln $(A_\infty A_t) = -k_{obst} + C$. The plots of k_{obs} versus the aniline concentration were linear passing through the origin, indicating that the reaction is second order with the absence of catalysis by the amine. Thus, second-order rate constants correspond to the overall rate constant (k_{tot}). Table II summarizes the kinetic results for the

Table I Percentage of Anilinium Picrate (% CO–O) in the Reaction Mixture of Aniline with Esters **1a–g** at Different Temperatures (20–40 °C) Using HPLC Measurements[a]

	Percentage of Anilinium Picrate (% CO–O)				
x	20°C	25°C	30°C	35°C	40°C
H	87.3	87.3	87.3	87.3	87.3
4-OMe	72.0	72.0	72.0	72.0	72.0
4-Me	78.3	78.3	78.3	78.3	78.3
3-Me	82.7	82.7	82.7	82.7	82.7
4-Cl	92.6	92.6	92.6	92.6	92.6
3-Cl	93.3	93.3	93.3	93.3	93.3
4-NO2	96.8	96.8	96.8	96.8	96.8

[a]The percentage of the *N*-phenyl picramide (% Ar–O) is the complementary percentage to 100 %.

Table II Total Second Order Rate Constants (k_{tot}) for the Reaction of Aniline and Picrylbenzoate Derivatives **1a–g**

		k_{tot} ($\times 10^2$ L mol^{-1} s^{-1}]				
Compound	x	20°C	25°C	30°C	35°C	40°C
3a	H	3.61	4.48	5.62	7.14	9.24
3b	4-OMe	1.00	1.41	2.00	2.86	4.14
3c	4-Me	1.61	2.19	3.00	4.14	5.75
3d	3-Me	2.55	3.33	4.39	5.81	7.79
3e	4-Cl	8.90	10.47	12.42	14.91	18.18
3f	3-Cl	15.60	18.36	21.25	24.58	28.48
3g	4-NO_2	80.66	88.02	96.02	104.77	114.44

$k_{tot,}$ is the second-order rate constants for the sum of C_{CO-O} and C_{Ar-O} cleavage.

Table III The Energies of Frontier Molecular Orbitals and the Esters **1a–g**, Aniline Evaluated by Using the B3LYP/6-31G ** Method

	$HOMO_{(ev)}$	$LUMO_{(ev)}$	ΔE^a (LUMO-HOMO)
H	– 7.5267[b]	– 3.4504[b]	1.94
4-OCH_3	– 6.7827[b]	– 3.3489[b]	2.05
4-CH_3	– 7.3035[b]	– 3.4019[b]	1.99
3-CH_3	– 7.2031[b]	– 3.424[b]	1.97
4-Cl	– 7.5035[b]	– 3.5464[b]	1.85
3-Cl	– 7.398[b]	– 3.5663[b]	1.83
4-NO_2	– 8.2203[b]	– 3.7535[b]	1.64
Aniline	– 5.39	0.23	

[a]LUMO (**a–g**) − HOMO (aniline).
[b]Ref. [10].

reactions of aniline with **1a–g** in methanol at different temperatures.

Effect of the Benzoyl Substituent on Reactivity. The kinetic data presented in Table II indicate that the reactivity of the titled esters toward the anilinolysis reaction follows the order 4-NO_2 > 3-Cl > 4-Cl > H > 3-Me > 4-Me > 4-OMe, meaning that the reactivity is inversely related to the electron donor ability of the substituent in the benzoyl moiety. Recently, in our previous work, we have reported that the DFT (B3LYB/6-31G**) calculated energies of the highest occupied molecular orbital (HOMO) and lowest unoccupied molecular orbital (LUMO) energy levels for the titled esters **1a–g** are affected by the change in the substituent in the benzoyl moiety [10], as shown in Table III. To get further insight into the effect of the benzoyl substituent on the reactivity, the authors extend the DFT calculations to aniline at the same level of theory, which are also shown in Table III. The comparison between the energies of the HOMOs of the esters **1a–g** and aniline shows that aniline has the highest-lying one. Thus, aniline acts as a donor molecule whereas the esters **1a–g** have low-lying LUMOs relative to aniline that is, they act as acceptor molecules, as shown in Fig 1. According to the perturbation theory, when the donor and the acceptor molecules approach each other their frontier molecular orbitals (FMOs) interact, resulting in bonding of the orbitals of the product. Actually, these interactions are stronger, when the FMO energies of the nucleophile and electrophile are closer. Thus the chemical reactivity of these esters toward the anilinolysis reaction is inversely proportional to the energy gap between the LUMO of the acceptor molecule (esters) and the HOMO of the donor molecule (aniline), that is, the reactivity increases with the decrease in the energy gap.

The calculations revealed that the energy gap follows the order 4-NO_2 < 3-Cl < 4-Cl < H < 3-Me < 4-Me < 4-OMe, which explains that the reactivity follows the reverse order.

In another treatment, the Hammett linear correlation, with a negative slope between the calculated energy gap and σ-Hammett constants of the benzoyl substituents (gradient = –0.37, r = 0 .992) indicates that electron-withdrawing substituents such as 4-NO_2, 3-Cl, and 4-Cl cause a decrease in the energy gap, reflecting a greater reactivity. However electron-donating substituents such as 3-Me, 4-Me, and 4-OMe show a

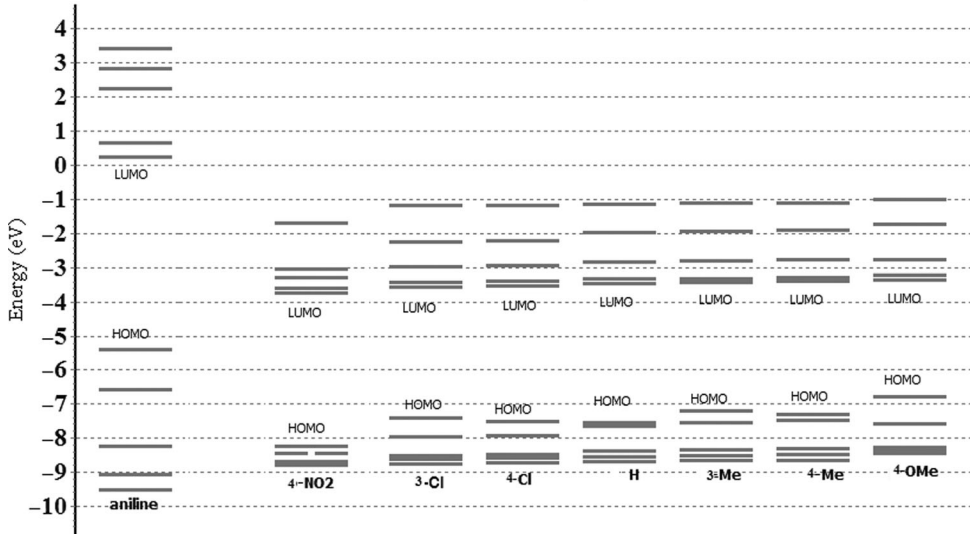

Figure 1 Simplified molecular orbital diagram for compounds **(1a-g)** and aniline.

decrease in the rate compared to the unsubstituted ester **1a** due to an increase in the energy gap. Furthermore, the linear relationship between the rate of anilinolysis and the computed values of the dipole moment of esters **1a–g** taken from [10] (gradient = –0.38, $r = 0.95$ at 25°C, except for (**1e**, X = 4-Cl) reveals that the decrease in the dipole moment of the substrate increases its reactivity toward aniline. This may be due to the fact that a dipole perturbs the electronic arrangement at the reaction sites [13a–13c].

Regioselectivity. In a previous study, the authors calculated the effective atomic charges with the usage of both Mulliken and natural bond orbital and the atomic orbital coefficient of LUMO calculated using the B3LYP method for the esters **1a–g**. The charges and the coefficient of each compound are confined to the two centers for the nucleophilic substitution reaction, namely the carbonyl carbon and ipso carbon. The calculations prove that the carbonyl carbon C7 is the hard electrophilic center whereas the ipso carbon is the soft one [10]. As a result, the authors have concluded that the regioselectivity of the nucleophilic reaction on the titled esters **1a–g** depends on the softness or hardness of the attacking nucleophile. When a hard nucleophile that has low-lying HOMO and is usually negatively charged is used, the reaction is referred to as charge controlled and would occur selectively on the carbonyl carbon and it will be kinetically fast due to a large electrostatic attraction. However, concerning the soft nucleophiles that have high-lying HOMO and do not necessarily have a negative charge, the reaction is referred to as FMO controlled and would occur selectively on the ipso carbon of the trinitrophenyl ring. Nevertheless, the interactions on each center, namely the carbonyl carbon or ipso carbon, can exhibit a mixture of charge and FMO contributions to intermediate-lying HOMO nucleophiles.

In the present study, the reagent of low polarizability such as aniline and at the same time is known as relatively "hard" nucleophile is inclined to attack the carbonyl carbon atom with the occurrence of CO–O cleavage. Meanwhile, the unexpected results of the aryl-oxygen cleavage ratio besides the predominant acyl-oxygen cleavage for the titled reaction are possibly due to the fact that the C-1 (ipso) of **1a–g** has high coefficient of atomic orbital than that of the carbonyl function of these esters [10]. This favors London forces being operative between the aniline and the high polarizable C-1 of the phenol moiety, leading to a minor aryl-oxygen cleavage process [7].

Furthermore, the low amount of aryl-oxygen cleavage can be attributed to the fact that the leaving group ability of picrate anions is higher than that of benzoates. This is corroborated by the fact that in methanol picric acid is a relatively strong acid, with $pK_a = 3.74$ at 25°C, whereas benzoic acid with $pK_a = 9.38$ [14]. Finally, inspection of Table II shows that the reaction temperature is another factor that controls the regioselectivity of the anilinolysis reaction, whereas the product formed due to acyl-oxygen cleavage (route a) is predominant at low temperature (20°C). On the other side, at higher temperature the products of aryl-oxygen cleavage (route b) have considerable amounts.

Mechanism and Reactivity for the Reaction of Aniline at the Acyl Site of the Esters 1a–g (Nucleophilic Acyl Substitution Reaction)

The second-order rate constant for the CO–O bond cleavage process (k_{CO-O}) was calculated by multiplying the overall rate constant k_{tot} by the experimentally determined fraction of CO–O, as shown in Table IV.

Table IV Rate Constant (k_{CO-O}) and Activation Parameters for Anilinolysis of Esters **1a–g** by Acyl-Oxygen Fission

		k_A ($\times 10^2$ L mol^{-1} s^{-1}]					Activation Parameters		
Compound	x	20°	25°	30°	35°	40°	$\Delta H^{\#}$ (kcal mol^{-1})	$-\Delta S^{\#}$ (cal mol^{-1} K^{-1})	$\Delta G^{\#}$ (kcal mol^{-1})
3a	H	3.15	3.70	4.32	5.02	5.81	4.97	48.36	20.34
3b	4-OMe	0.72	0.92	1.16	1.45	1.80	7.73	41.86	20.60
3c	4-Me	1.26	1.59	1.99	2.48	3.06	7.50	41.54	20.50
3d	3-Me	2.16	2.66	3.27	3.98	4.82	6.71	43.16	20.43
3e	4-Cl	8.24	9.35	10.57	11.90	13.35	3.79	50.47	20.13
3f	3-Cl	14.55	16.49	18.62	20.93	23.46	3.75	49.49	19.94
3g	4-NO_2	78.11	84.42	91.00	97.85	104.98	2.09	51.82	19.53
	ρ	1.86	1.80	1.74	1.69	1.63			
	R	0.989	0.992	0.994	0.996	0.997			

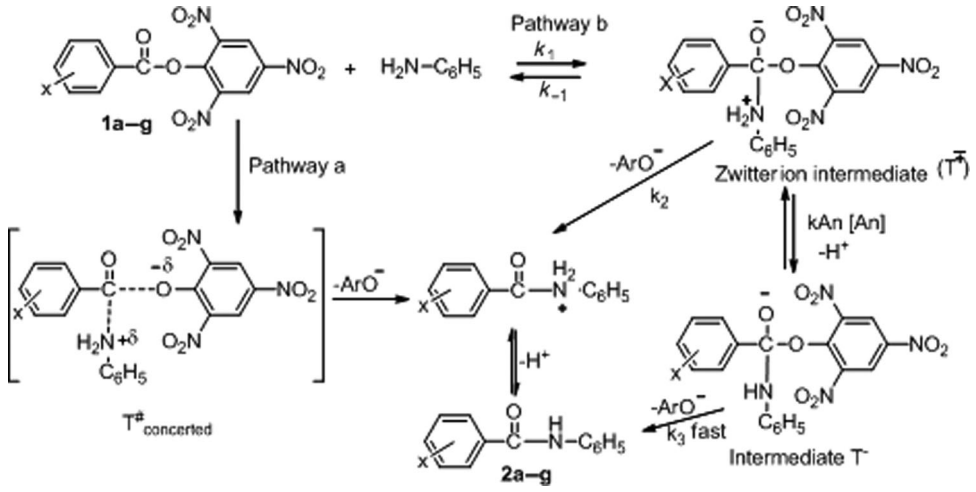

Scheme 2 Ar = 2,4,6-trinitrophenyl; a, x = H; b, x = 4-OMe; c, x = 4-Me; d, x = 3-Me; e, x = 4-Cl; f, x = 3-Cl; g, x = 4-NO_2.

The mechanism of anilinolysis of esters **1a–g** at the acyl site can proceed by either a concerted process (pathway a) or a stepwise mechanism (pathway b). The stepwise mechanism could involve two reaction pathways: the uncatalyzed reaction with an overall second order, k_2, and the catalyzed reaction by aniline with an overall third order, k_3 (Scheme 2).

In the stepwise mechanism (pathway b), the aniline molecule first attacks the carbonyl carbon of a reactant to form a tetrahedral intermediate and then it decomposes to generate products **2a–g** and Ar'O$^-$ as shown in Scheme 2.The possibility of the reaction to proceed by aniline catalysis is rejected on the ground that the reaction is second order.

In the present study, the correlation of second-order rate coefficients with Hammett substituent constants yields a linear straight line with positive slope. Hence, such a linear plot clearly indicates that the reaction at the carbonyl group of the ester **1a–g** proceeds without changing the rate-determining step and proves that changing the electronic nature of the substituent in the nonleaving group does not change the reaction mechanism. The large ρ values exclude the concerted mechanism [15] and are in accordance with those values found for the stepwise mechanism in which the rate-limiting step is the formation of the tetrahedral intermediate (Scheme 2, pathway b). In fact, this is the case of the reactions of 4-nitrophenyl x substituted benzoates with anionic nucleophiles [16].

Since all the substituents are located in para or meta position, a direct steric interaction is unlikely and resonance and/or inductive effects are the operating factors. This suggested mechanism is consistent with the explanation that an electron-withdrawing substituent, for example, NO_2, **1g**, would accelerate the rate of reaction, but would retard the rate of the leaving group on departure. The authors ascribed the enhancement in the rate to the increase in the electrophilicity of the carbonyl carbon and the presence of the NO_2 group that stabilizes the tetrahedral intermediate T$^-$. In contrast, an electron-donating substituent for example, 4-OMe, **1b**, would inhibit nucleophilic attack but would increase the rate at which the leaving group departs. One can suggest that the ground-state stabilization through the resonance interaction as illustrated in the resonance structures (I–IV) is responsible for the low reactivity shown by the substrate with an EDG (e.g., X = 4-OMe) as shown in Fig 2.

The values of $\Delta H^{\#}$ and $\Delta S^{\#}$ for the reaction of aniline at the carbonyl carbon center of the ester **1a–g** are, respectively, obtained from the slope and intercept of Eyring plots by the least-squares analysis, as shown in Table IV. Although the low positive $\Delta H^{\#}$ and large negative $\Delta S^{\#}$ values are in line with the stepwise mechanism, they can also be interpreted as supportive of a concerted mechanism. The plots of $\Delta S^{\#}$ versus $\Delta H^{\#}$ values (not shown) for the nucleophilic acyl substitution gave a straight line with isokinetic temperature –272.5°C (the temperature at which the substituent effects are supposed to be reversed). This linear relationship indicated a common mechanism for all substituents and independent of its nature and position as well as the value is far from the temperatures used in the kinetic runs [17]. The constancy of $\Delta G^{\#}$ may be explained on the basis of an isokinetic

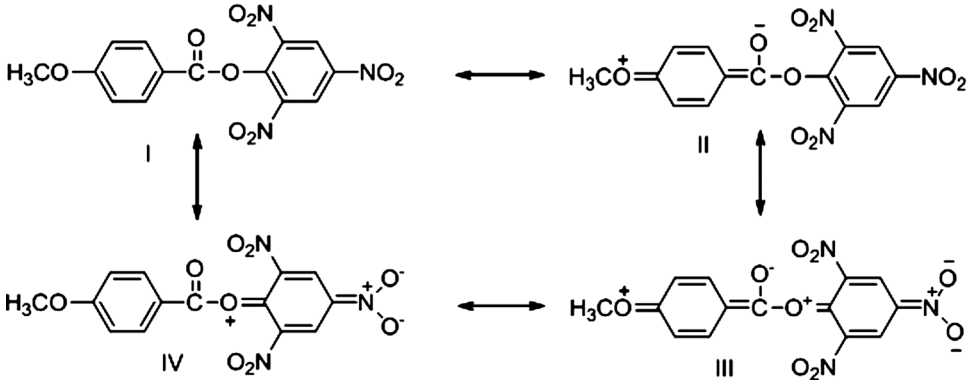

Figure 2 Ground state stabilization through resonance for compound **1g**.

relationship that exists for a series of esters of slightly different structures but undergoing a reaction essentially by the same mechanism.

Mechanism and Reactivity for the Reaction of Aniline at the Ipso Site of the Esters 1a–g (Nucleophilic Aromatic Substitution Reaction)

Aromatic nucleophilic substitution reactions have been proposed to proceed through an addition-elimination mechanism (Ad-E; S_NAr) involving the formation of Meisenheimer and zwitterionic complexes [18]. As a matter of fact, previous mechanistic investigations have included examination of the effects of nucleophilic strength, solvation [19–22], leaving group ability, and reactivity of the substrates [23–25]. There has been a discourse on whether the rate-determining step is the addition of the nucleophile, elimination of the leaving group [26], proton transfer process [27], or whether it may switch depending on the solvent, nature of the nucleophile, the steric factor, as well as the degree of activation of the aromatic substrate, and the relative position of activating substitution(s) to the reaction center [18,28]. The second-order rate constants for the reaction at the ipso carbon of the phenolic moiety ($k_{Ar–O}$) are calculated by subtracting the rate corresponding to acyl oxygen cleavage from the total rate coefficients, as shown in Table V.

It has been well known that S_NAr reactions proceed through a zwitterion intermediate, in which the rate-determining step can either form or break down the intermediate, as shown in Scheme 3.

If the departure of the leaving group from the zwitterionic intermediate occurs in the rate-determining step, the magnitude of the $k_{Ar–O}$ should increase linearly with increasing the electron-withdrawing ability of the substituent x in the leaving benzoyl moiety. However, as shown in Table IV, the $k_{Ar–O}$ values have small difference upon changing the substituent x from a strong EDG (e.g., 4-MeO) to a strong EWG (e.g., 4-NO_2) even though 4-NO_2 shows a slightly high value. Therefore,

Table V Rate Constant ($k_{Ar–O}$) and Activation Parameters for Anilinolysis of Esters **1a-g** by Aryl-Oxygen Fission

	$k_{Ar–O}$ ($\times 10^2$ L mol^{-1} s^{-1}]					Activation parameters		
x	20°C	25°C	30°C	35°C	40°C	$\Delta H^{\#}$ (kcal mol^{-1})	$-\Delta S^{\#}$ (cal mol^{-1} K^{-1})	pK_a (H_2O) [29]
H	0.46	0.78	1.30	2.12	3.43	17.68	8.80	4.20
4-OMe	0.28	0.49	0.84	1.41	2.34	18.71	6.25	4.47
4-Me	0.35	0.60	1.01	1.66	2.69	17.97	8.37	4.36
3-Me	0.39	0.67	1.12	1.83	2.97	17.85	8.53	4.27
4-Cl	0.66	1.12	1.85	3.01	4.83	17.50	8.69	3.99
3-Cl	1.05	1.87	2.63	3.65	5.02	13.26	22.07	3.83
4-NO_2	2.55	3.60	5.02	6.92	9.46	11.33	27.07	3.44
ρ	0.92	0.85	0.75	0.65	0.56			
R	0.990	0.986	0.996	0.998	0.988			

pK_a values for the conjugate substituted benzoic acids of the X-benzoate leaving groups in water are taken from [29].

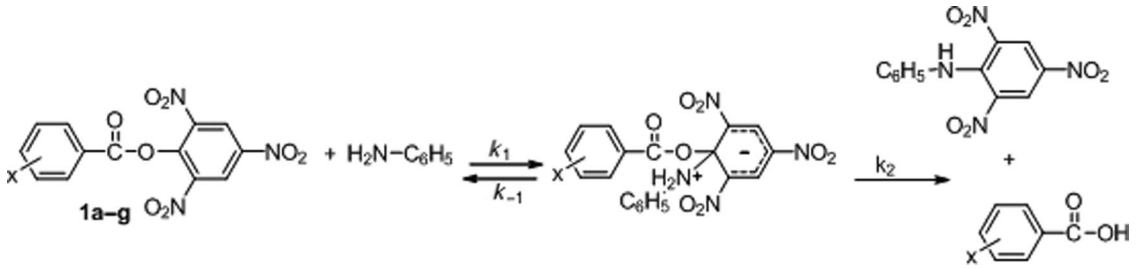

Scheme 3 a, x = H; b, x = 4-OMe; c, x = 4-Me; d, x = 3-Me; e, x = 4-Cl; f, x = 3-Cl; g, x = 4-NO_2.

the present result clearly suggests that the Ar–O bond cleavage proceeds through a S_NAr mechanism in which the departure of the leaving group from the zwitterion intermediate occurs rapidly after the rate-determining step, as shown in Scheme 3.

The Hammett correlation with σ-constants exhibits a good linear relationship with a relatively small slope (ρ = 0.92–0.56) for the reaction of **1a–g** with aniline at the ipso site, as shown in Table V. These low values of ρ for aryl-oxygen cleavage is in contrast to the previously reported value (ca. +4) [3] for substituted halogenonitrobenzene, which can be explained on the basis that substituents of halogenonitrobenzene directly affect the reaction center; on the other hand, in this study, the substituents exist in the leaving group benzoyl moiety. In addition, it is observed that the ρ values are far poorer than those for the acyl-oxygen cleavage reaction. One might suggest two possible reasons for these differences between ρ values of the two reaction routes: (i) The nature of the reaction mechanism would be responsible for the insignificance of the substituent effect on the $k_{Ar–O}$ value, where the bulk of the negative charge is delocalized conjugatively into the trinitrophenyl ring when the reaction undergoes aryl-oxygen cleavage, whereas the localized negative charge is greatly affected by x substituent when the ester undergoes acyl-oxygen cleavage. (ii) The proximity effect, the reaction site of the Ar–O bond cleavage is far from the substituent X in the benzoyl moiety by two atoms than that of the CO–O bond cleavage. Since the inductive effect of the substituent diminishes with the distance between the substituent and the reaction site, so the effect of the benzoyl substituent would be less significant for the Ar–O bond cleavage than for the CO–O bond cleavage process.

The Brönsted relationship has been used as a probe for determining the mechanistic pathway [30,31]. The magnitude of the Brönsted coefficient has usually been related to the extent of the bond formation in the transition state, and when an intermediate is formed along the reaction pathway a large Brönsted coefficient is expected [31]. Table V illustrates that the reactivity of picryl benzoate derivatives **1a–g** toward aniline increases with the decrease in pK_a of the benzoic leaving group. The relatively small β_{lg} value (–0.93, r = 0.99) obtained in our study assists our assumption that the reaction of **1a–g** proceeds through a zwitterion intermediate in which bond formation to the nucleophile is well advanced, and bond breaking to the leaving group has proceeded in a negligible extent in the transition state.

The values of the activation enthalpy demonstrate a small difference with changing substituent in the ester **1a–g**, as shown in Table V. On the other hand, all types of substituents show negative entropy of activation. The plot of $\Delta S^{\#}$ versus $\Delta H^{\#}$ for the nucleophilic aryl substitution gave a straight line with isokinetic temperature –272.81°C, which is far from the temperatures used in the kinetic runs. This linear plot indicates a common mechanism for all substituents and is independent of its nature and position. The calculations revealed that the esters have negative entropy and pronounced in (4-NO_2, 3-Cl); that is, the transition state is more organized than the reactants.

CONCLUSIONS

The present study has allowed us to conclude the following:

1. The anilinolysis of picryl x substituted benzoate **1a–g** proceeds via simultaneous acyl-oxygen and aryl-oxygen fissions under the reaction temperature used in this study.
2. The reactivity of these esters toward anilinolysis is inversely proportional to the energy gap calculated between HOMO aniline and LUMO for each ester.
3. The product formed due to acyl-oxygen fission is the predominant product, which can be explained on the basis that aniline is relatively hard nucleophile and picrate anion is a good leaving group compared to benzoate anions.

4. The mechanism of acyl-oxygen fission proceeds through the stepwise mechanism in which the formation of the tetrahedral intermediate is the rate-determining step. The aryl-oxygen bond cleavage proceeds through a S_NAr mechanism in which the departure of the leaving group from the Meisenheimer complex occurs rapidly after its formation in the rate-limiting step.

BIBLIOGRAPHY

1. (a) Fewer, H. In The Chemistry of the Nitro and Nitroso Groups; Patai, S., Ed.; Interscience: New York, 1969; (b) Buncel, E.; Chuaqui, C.; Forsythe, P.; Mahoney, S.; Raoult, A.; Willtshir, J.F. J Chem Soc, Perkin II 1975, 478–482.
2. (a) Kirby, A. J.; Jencks, W.P J Am Chem Soc 1965, 87, 3209–3216; (b) Benkovic, S.J.; Benkovic, B. A. J Am Chem Soc 1966, 88, 5504–5511.
3. (a) Kirby, A. J. In Comprehensive Chemical Kinetics; Bamford, C. H.; Tipper, C. F. H., Eds.; Elsevier: Amsterdam, 1972; (b) Bender, M. L. Mechanisms of Homogeneous Catalysis from Protons to Proteins; Wiley-Interscience: New York, 1971.
4. Guanti, G.; Dell'Erba, C.; Pero, F.; Leandri, G. J Chem Soc, Chem Commun 1975, 823–824.
5. Kirsch, J. F.; Clewell, W.; Simon, A. J Org Chem 1968, 33, 127–132.
6. Konasiewicz, A.K.; Maccoll, A. J Chem Sec 1964, 1267–1274.
7. Guanti, G.; Dell'Erba, C.; Pero, F.; Leandri, G. J Chem Soc, Perkin II 1977, 966–970.
8. Edwards, J. O.; Pearson, R.G. Hard and Soft Acids and Bases; Pearson, R. G., Eds.; Dowden, Hutchinson, Ross: Stroudsburg, PA, 1973.
9. (a) Bach, R. D.; Coddens, B. A.; Wolber, G. J. J Org Chem 1986, 51, 1030–1033; (b) Rajeshwar, R. B. Ind J Chem B 2002, 41, 1694–1696; (c) De, B. R.; Maity, M.; Mahato, S.; Saw, K. Ind J Chem A 2003, 42, 1622–1626. (d) Tanaka, K.; Deguchi, M.; Iwata, S. J Chem Res, Synop 1999, 528–529.
10. Fawzy, M. F.; Senior, S.; El-Atawy, M. A.; El-Sadany, S. K.; Hamed, E. A. J Mol Struct 2011, 1006, 303–311.
11. Frisch, M. J.; Trucks, G. W.; Schlegel, H. B.; Scuseria, G. E.; Robb, M. A.; Cheeseman, J. R.; Zakrzewski, V. G.; Montgomery, J. A., Jr.; Stratmann, R. E.; Burant, J. C.; Dapprich, S.; Millam, J. M.; Daniels, A. D.; Kudin, K. N.; Farkas, O.; Tomasi, J.; Barone, V.; Cossi, M.; Cammi, R.; Pomelli, C.; Adamo, C.; Clifford, S.; Ochterski, J.; Petersson, G. A.; Cui, Q.; Morokuma, K.; Malick, D. K.; Rabuck, A. D.; Foresman, J. B.; Cioslowski, J.; Ortiz, J. V.; Baboul, A. G.; Stefanov, B. B.; Liu, G.; Liashenko, A.; Piskorz, P.; Komaromi, I.; Gomperts, R.; Fox, D. J.; Keith, T.; Al-Laham, M. A.; Peng, C. Y.; Anayakkara, A.; Challacombe, M.; Gill, P. M. W.; Johnson, B.; Chen, W.; Wong, M. W.; Andres, J. L.; Gonzalez, C.; Head-Gordon, M.; Replogle, E. S.; Pople, J. A. Gaussian 98; Gaussian, Inc.: Pittsburgh, PA, 1998
12. (a) Becke, D. J Chem Phys 1993, 98, 5648–5652; (b) Lee, C.; Yang, W.; Parr R. G. Phys Rev B 1988, 37, 785–789; (c) Hariharan, P. C.; Pople J. A. Chem Phys Lett 1972, 16, 217–219.
13. (a) Um, I-H.; Park, Y-M.; Fujio, M.; Mishima, M.; Tsuno, Y. J Org Chem 2007, 72, 4816–4821, and the references therein; (b) Reddy, S. R.; Rajeswara Rao, B.; Manikyamba, P. Ind J Chem 2007, 46A, 436–439; (c) Kilpatrick, M.; Arenberg, C. A. J Am Chem Soc 1953, 75, 3812–3821.
14. Um, I. H.; Lee, J. Y.; Fujio, M.; Tsuno, Y., Org Biomol Chem 2006, 4, 2979–2985.
15. Leffler, J. E. J Org Chem 1955, 20, 1202–1231.
16. Miller, J. Aromatic Nucleophilic Substitution; Elsevier: Amsterdam, 1968.
17. (a) Jose, K. B.; Gyriac, J.; Moolayil, J. T.; Sebastian, V. S.; George, M. J Phys Org Chem 2011, 24, 714–719; (b) Alvaro, C. E. S.; Nudelman, N. S., Arkivoc 2003, 95–106.
18. Acevedo, O.; Jorgensen, W. L. Org Lett 2004, 6, 2881–2884.
19. (a) Paghaleh, J.; Harifi-Mood, A. R. J Phys Org Chem 2011, 24, 1095–1100; (b) Fathalla, M. F., Int J Chem Kinet 2006, 38, 159–165.
20. (a) El-Mallah, N. M.; Senior, S. A.; Nabil, G. M.; Ramadan, M. S.; Hamed, E. A. Int J Chem Kinet 2010, 42 453–463; (b) Fathalla, M. F.; Hamed, E. A. J Chem Res 2006, 413–416.
21. (a) Crampton, M. R.; Emokpae, T. A.; Howard, J. A. K.; Isanbor, C.; Mondal, R. J Phys Org Chem 2004, 17, 65–70; (b) Fathalla, M. F.; Ibrahim, M. F.; Hamed, E. A. J Chem Res 2004, 150–151.
22. Al-Howsaway, H. O. H.; Fathalla, M. F.; El. Bordan, A. A.; Hamed, E. A. J Chem Res 2007, 509–512.
23. Crampton, M. R.; Emokpae, T. A.; Isanbor, C. Eur J Org Chem 2007, 1378–1383.
24. Hasegawa, Y. J Chem Soc, Perkin Trans 2 1984, 547–551.
25. Chamberlain, R. A.; Crampton, M. R. J Chem Soc, Perkin Trans 2 1995, 1831–1838, and references therein.
26. Crampton, M. R.; Emokpae, T. A.; Isanbor, C.; Batsanov, A. S.; Howard, J. A. K.; Mondal, R. Eur J Org Chem 2006, 1222–1230, and references therein.
27. (a) Espinosa, S.; Bosch, E.; Rosés, M.; J Chromotogr 2002, 964, 55–66; (b) Dean, A. J. Lange's Handbook of Chemistry; McGraw Hill: New York, 2003; (c) Lide, D. R. CRC Handbook of Chemistry and Physics, 83rd Ed., CRC Press, 2002.
28. Mohanty, T. R.; Nayak, P. L. J Chem Soc, Perkin II 1975, 242–244.
29. Senator, L.; Ciuffarin, E.; Fava, A. J Am Chem Soc 1970, 92, 3035–3039.
30. El-Hegazy, F. E. M.; Abdel Fattah, S. Z.; Hamed, E. A.; Sharaf, S. M. J Phys Org Chem 2000, 13, 549–554, and references therein.
31. Khatab, S. N.; Hamed, E. A.; Albericio, F.; El-Faham, A. Bull Chem Soc Jpn 2011, 84, 633–63